



Ioannis V. Yentekakis
Laboratory of Physical Chemistry & Chemical Processes (www.pccplab.tuc.gr), School of Chemical & Environmental Engineering, Technical University of Crete, 73100-Chania, Crete, Greece

1. Abstract

- Effective promotion of catalytic reactions is always a grand challenge for heterogeneous catalysis [e.g., 1-3].
- As it has been well-established, the creation of an *effective-double-layer* (EDL) on catalyst particle surfaces imposed either through metal-support interactions or via an external bias application, is a unique, ultra-effective method for catalysts promotion [2, 4].
- Nevertheless, catalyst nanoparticles (NPs) stabilization at the typically elevated operation temperatures of catalysis is at least of equivalent, unless of much more importance, since sintering of NPs is inevitably a leading cause of catalysts degradation used for energy, environmental and large-scale synthesis of commodity chemicals applications with obvious economic drawbacks [5-7].
- We have recently discovered that the *effective-double-layer*, spontaneously created on catalyst nanoparticle surfaces via *metal-support* interactions with supports that have high lattice oxygen lability and mobility (Fig. 1), can play a critical, additional to activity promotion, role on providing sinter resistant catalysts; unprecedented stabilization of catalyst nanoparticles dispersed on such supports has been achieved [8-13].
- A plausible model (Fig. 3), based on the *effective-double-layer* approach for metal-support interactions (Figs. 1 and 2), which streamlines and convincingly interprets the observed resistance to sintering (even redispersion) of NPs in addition to selected experimental findings obtained so far in our laboratory on the subject that demonstrate the new phenomenon are presented herein.

2. Experimental methods

- Ir and Rh nanoparticles (~1 wt%) were dispersed, via wet impregnation, on oxide and mixed-oxide supports characterized by very different *oxygen storage capacities and labilities* (i.e., γ - Al_2O_3 , yttria stabilized zirconia (YSZ), alumina-ceria-zirconia (ACZ) and ceria-zirconia (CZ), gadolinia doped ceria (GDC)).
- The Oxygen Storage Capacity (OSC) values of the supports were estimated by using H_2 -TPR profiles obtained

3. Aspects of our EDL-based model deciphering the causes of the catalyst nanoparticles anti-sintering and/or redispersion behavior.

3.1. The spontaneous creation of the effective-double-layer (EDL: $[O^{\delta-}, \delta^+]$) when catalyst's nanoparticles are in ultimate contact with supports possessing high oxygen ion lability, and its possible roles in catalysis:

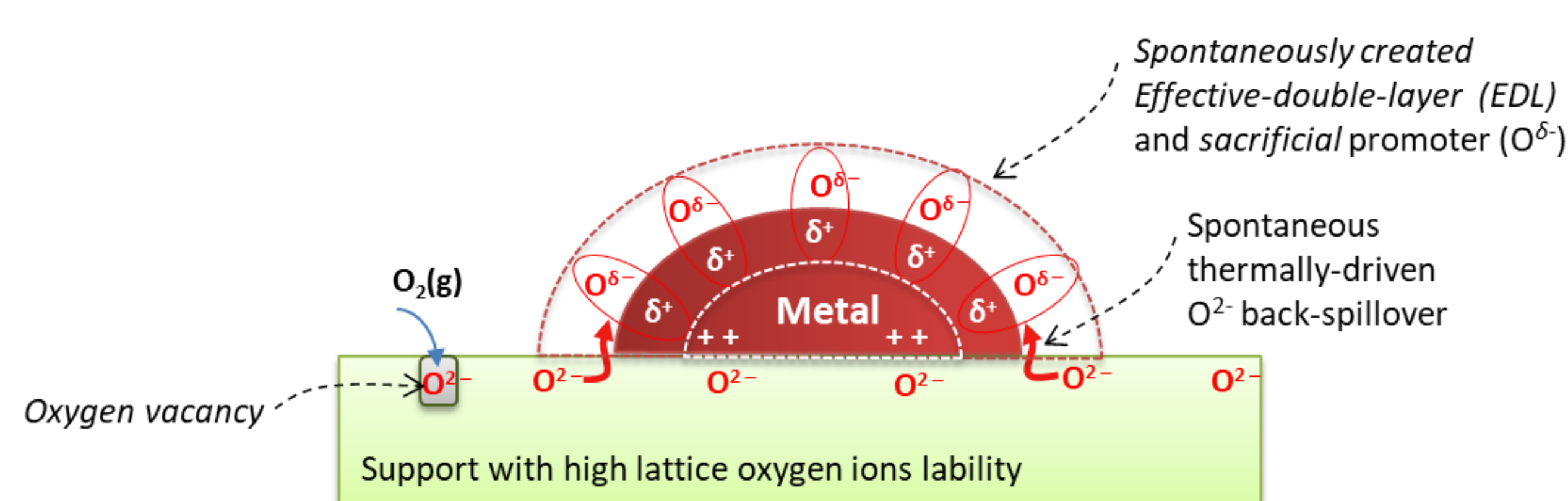


Fig. 1: Spontaneously created *effective-double-layer* via thermally driven O^{2-} ions back-spillover on catalyst nanoparticles dispersed on supports with high lattice oxygen ion lability and storage capacity (according to the theory described in refs. [2] and [4]).

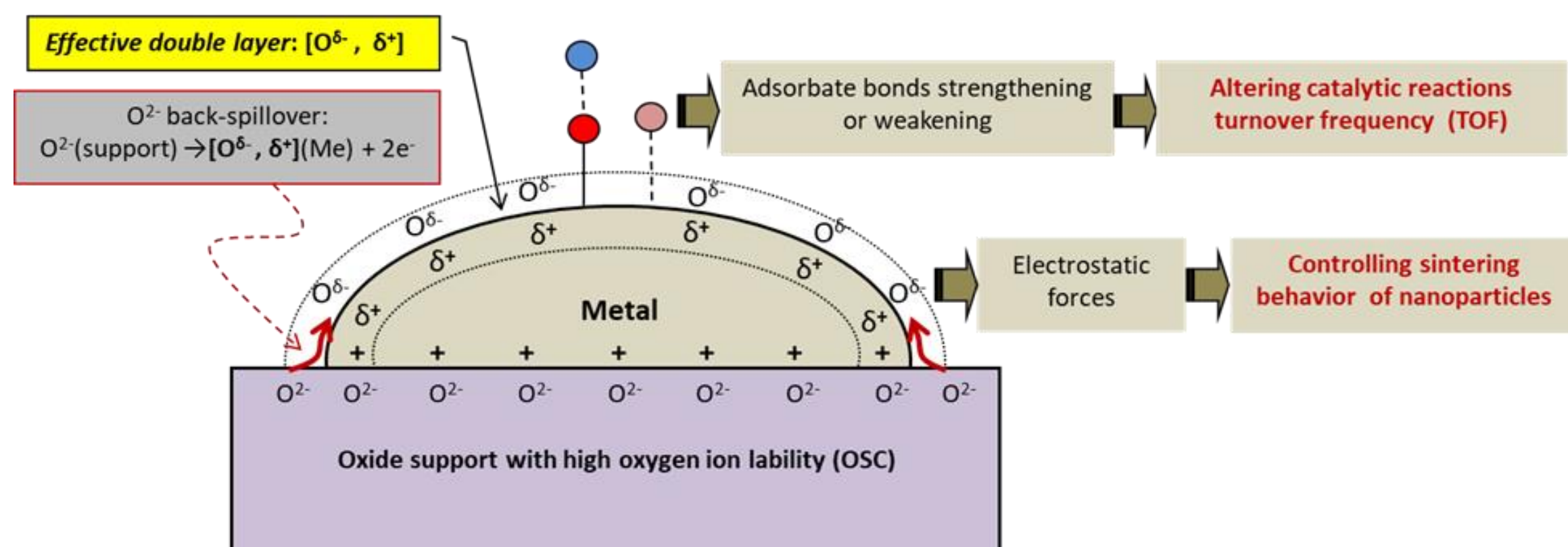


Fig. 2: The dual functional role of the *effective-double-layer* $[O^{\delta-}, \delta^+]$ in heterogeneous catalysis: promotion of the intrinsic catalytic activity and stabilization of catalyst nanostructure.

3.2. The EDL-based model for sinter-resistant and/or redispersion of catalyst nanoparticles:

- There are three main pathways (I, II and III in Fig. 3) associated with particle size growth and our model includes the key factors that are expected to control their contribution and intensity.
- Path I:** It concerns large particle migration and coalescence (PMC), which according to our model is considered to be strongly inhibited by electrostatic interparticle repulsion due to the presence of the EDL and the consequent coating of particles with a net negative charge ($O^{\delta-}$).
 - Path II (a) and (b):** It concerns the Ostwald ripening (OR) sequence, i.e., atom detachment (IIa) and reattachment (IIb), both of which are supposed to be inhibited by the increased activation energies resulting from the $O^{\delta-}$ -encapsulated particle surfaces.
 - Path III:** It concerns the diffusion of detached atomic species from smaller particles towards larger ones, which is strongly inhibited by atom trapping at surface oxygen vacancy (V_O) centers.

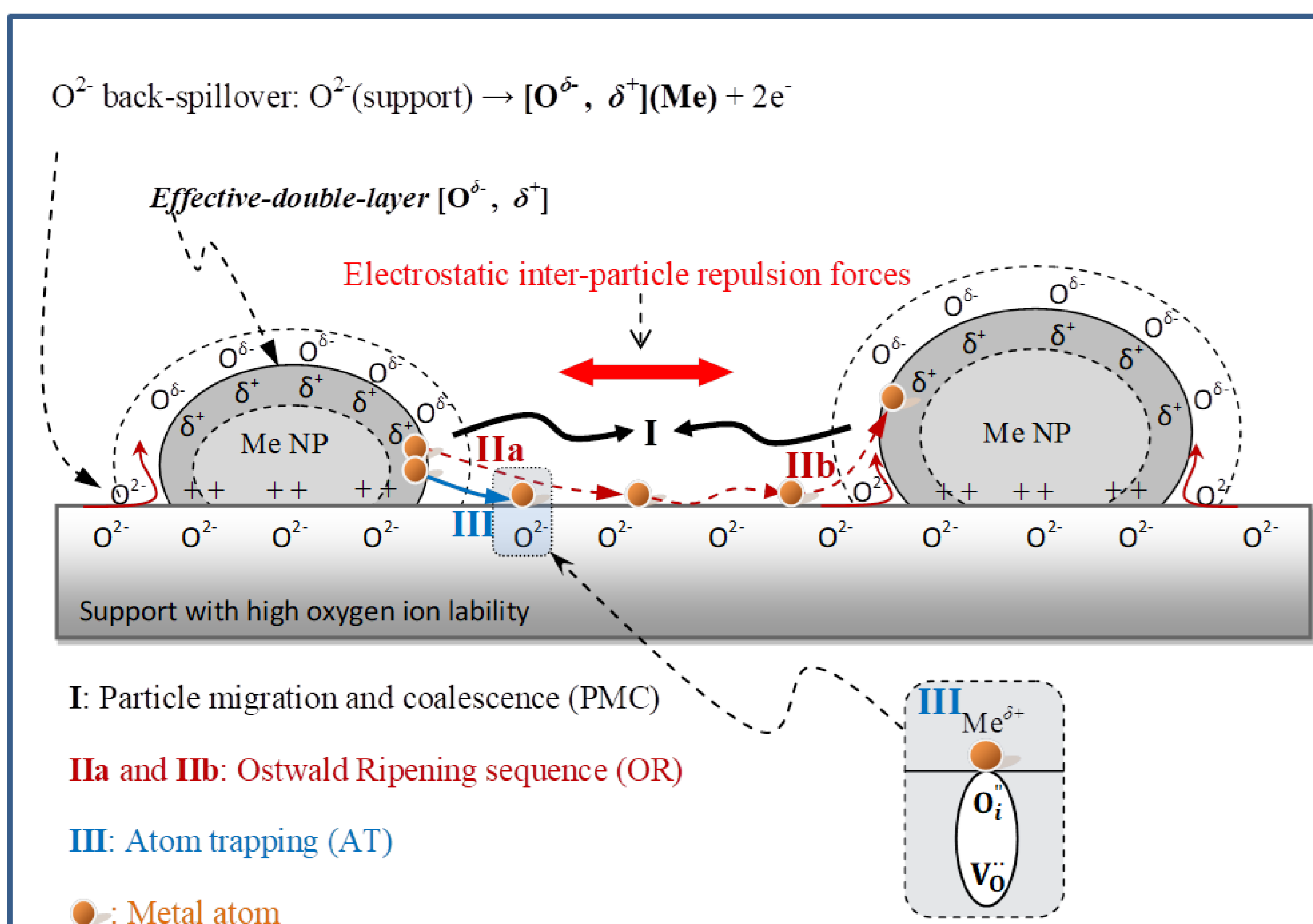


Fig. 3: Model deciphering the sintering resistance of dispersed catalyst nanoparticles against PMC and agglomeration mechanisms as well as redispersion phenomena, resulting from the simultaneous action of (i) the EDL and its subsequent interparticle repulsion forces and the suppression of detachment/reattachment of atom species, and (ii) the atom-trapping at support surface oxygen ion vacancies.

According to these factors proposed in our EDL-based model to be critical to the sintering behavior of the catalyst nanoparticles, the experimental findings (see below) can be consistently rationalized as follows.

- In the absence of the *effective-double-layer* (e.g., when γ - Al_2O_3 support is used) none of the above potential anti-sintering factors (I, II, and III) are at work to protect particle agglomeration; the obtained severe Ir and Rh nanoparticles agglomeration on Ir/ γ - Al_2O_3 (Fig. 5a and Rh/ γ - Al_2O_3 (Fig. 5b) catalysts is then easily understandable. The extent of agglomeration mainly depends on the nature of the metal particle (Ir is more sensitive to agglomerate than Rh).
- The presence of the *effective-double-layer*, with its accompanying effects on paths I and II, can lead to either moderate or substantial sinter protection (Fig. 5a), or even redispersion (Fig. 5b), depending on the intensity of the EDL and the transport properties of the metal particles (metal nature).

in the temperature region 25-850°C:

Supports	OSC ($\mu mol O_2/g$)
γ - Al_2O_3 (100% Al_2O_3)	0
YSZ (8 mol% Y_2O_3 - ZrO_2)	6
ACZ (80wt% Al_2O_3 -20wt% $Ce_{0.5}Zr_{0.5}O_{2.6}$)	110
GDC (10 mol% Gd_2O_3 - CeO_2)	186
CZ ($Ce_{0.5}Zr_{0.5}O_{2.6}$)	557

- Sintering performance of the as-prepared supported Ir and Rh catalysts was investigated on samples that underwent thermal aging at high temperatures (i.e., 750°C or 750°C + 850°C for 2h at each temperature) in oxidative environment (air). Nanoparticle sizes were estimated by the use of isothermal H_2 -chemisorption, and corroborated by HRTEM measurements on both fresh and sintered samples (Table 1).
- The catalyst nanoparticles growth and/or redispersion was calculated by using the following equation:
 $\% \text{ particle growth} = 100 \cdot (PS - PS^0) / PS^0$
where PS denotes mean metal particle size, and the superscript "0" refers to fresh (un-sintered) samples and plotted versus support's OSC (Fig. 5).
- A series of fresh and their sintered counterpart catalysts, namely Ir/ γ - Al_2O_3 , Ir/YSZ and Ir/GDC, were tested under a reaction of high environmental and energy importance, specifically the Dry Reforming of Methane (DRM) in order to exemplify and evaluate thermal aging stability of the catalysts according to the aforementioned EDL-governed anti-sintering and re-dispersion phenomena.

4. Experimental findings that led to the development of the model and agree with its predictions.

Table 1 Characteristics of fresh and sintered catalysts.

Catalysts	S_{BET} (m^2/g)	D_{metal} (%)	Mean metal particle size (nm) ^b H ₂ -chemTEM
Ir-based catalysts^a			
0.7wt% Ir/ γ - Al_2O_3 -fresh	159	88	0.8 / 1.2±0.4
0.7wt% Ir/ γ - Al_2O_3 -sinter@750	140	3	28.8 / 14.5±6.5
0.7wt% Ir/YSZ-fresh	4	33	2.2 / 1.2±0.4
0.7wt% Ir/YSZ-sinter@750	4	3	22.6 / 10.5±5.5
0.4wt% Ir/GDC-fresh	10	48	1.5 / 1.7±0.5
0.4wt% Ir/GDC-sinter@750	10	41	1.8 / 2.0±1.0
0.4wt% Ir/ACZ-fresh	73	41	1.8 / 1.6±0.5
0.4wt% Ir/ACZ-sinter@750	64	45	1.6 / 1.9±0.4
1.0wt% Ir/ γ - Al_2O_3 -fresh	167	70	1.0 / 1.2±0.3
1.0wt% Ir/ γ - Al_2O_3 -sinter@750	140	5	13.6 / n.m.
0.4wt% Ir/ACZ-fresh	73	41	1.7 / 1.8±0.5
0.04wt% Ir/ACZ-sinter@750	64	34	2.1 / n.m.
0.6wt% Ir/CZ-fresh	17	61	1.2 / 1.3±0.4
0.6wt% Ir/CZ-sinter@750	16	44	1.6 / n.m.
Rh-based catalysts^a			
1.0wt% Rh/ γ - Al_2O_3 -fresh	160	88	1.2 / 1.3±0.4
1.0wt% Rh/ γ - Al_2O_3 -sinter@750	159	69	1.6 / 1.6±0.3
1.0wt% Rh/ γ - Al_2O_3 -sinter@850	140	41	2.6 / 1.6±0.3
0.8wt% Rh/ACZ-fresh	136	77	1.8 / 1.5±0.5
0.8wt% Rh/ACZ-sinter@750	n.m.	91	1.4 / 2.0±0.8
0.8wt% Rh/ACZ-sinter@850	n.m.	81	1.7 / 1.5±0.4
0.8wt% Rh/CZ-fresh	17	27	5.0 / 5.1±1.7
0.8wt% Rh/CZ-sinter@750	12	65	2.1 / 2.5±0.7
0.8wt% Rh/CZ-sinter@850	n.m.	62	2.2 / 2.0±0.7

^a Ir and Rh contents were measured via ICP-OES.

^b The mean metal particle size compare values estimated via H₂-Chemisorption and HRTEM

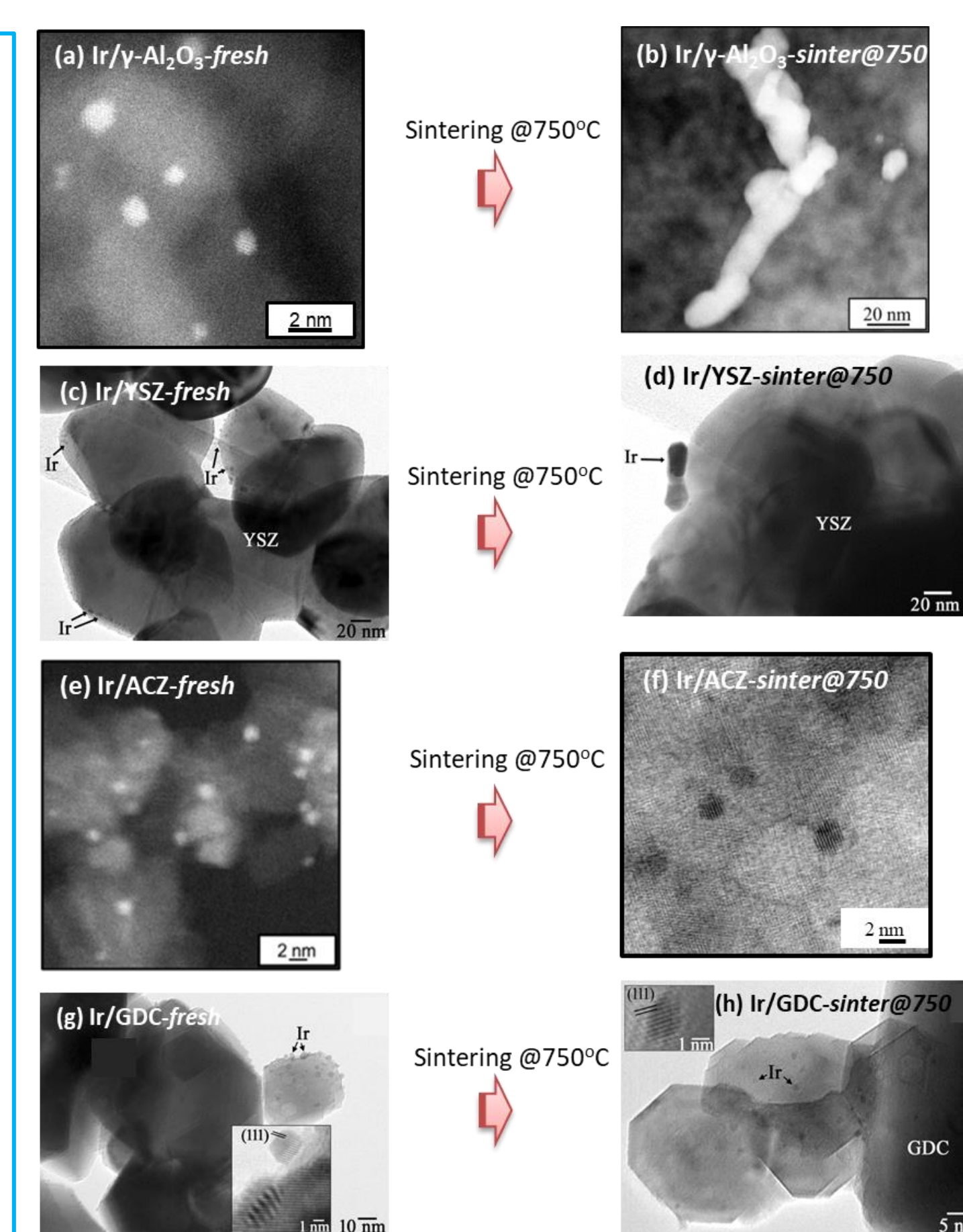


Fig. 4: HRTEM images of the fresh (a, c, e, g) and sinter@750 (b, d, f, h) Ir/ γ - Al_2O_3 , Ir/YSZ, Ir/ACZ and Ir/GDC catalysts, respectively. The particle size of Ir NPs supported on high oxygen ion lability supports (ACZ and GDC) remains almost constant in opposite to Ir NPs supported on negligible oxygen ion lability supports (γ - Al_2O_3 and YSZ) where a substantial agglomeration is resulted after the high temperature treatment [8,9,10].

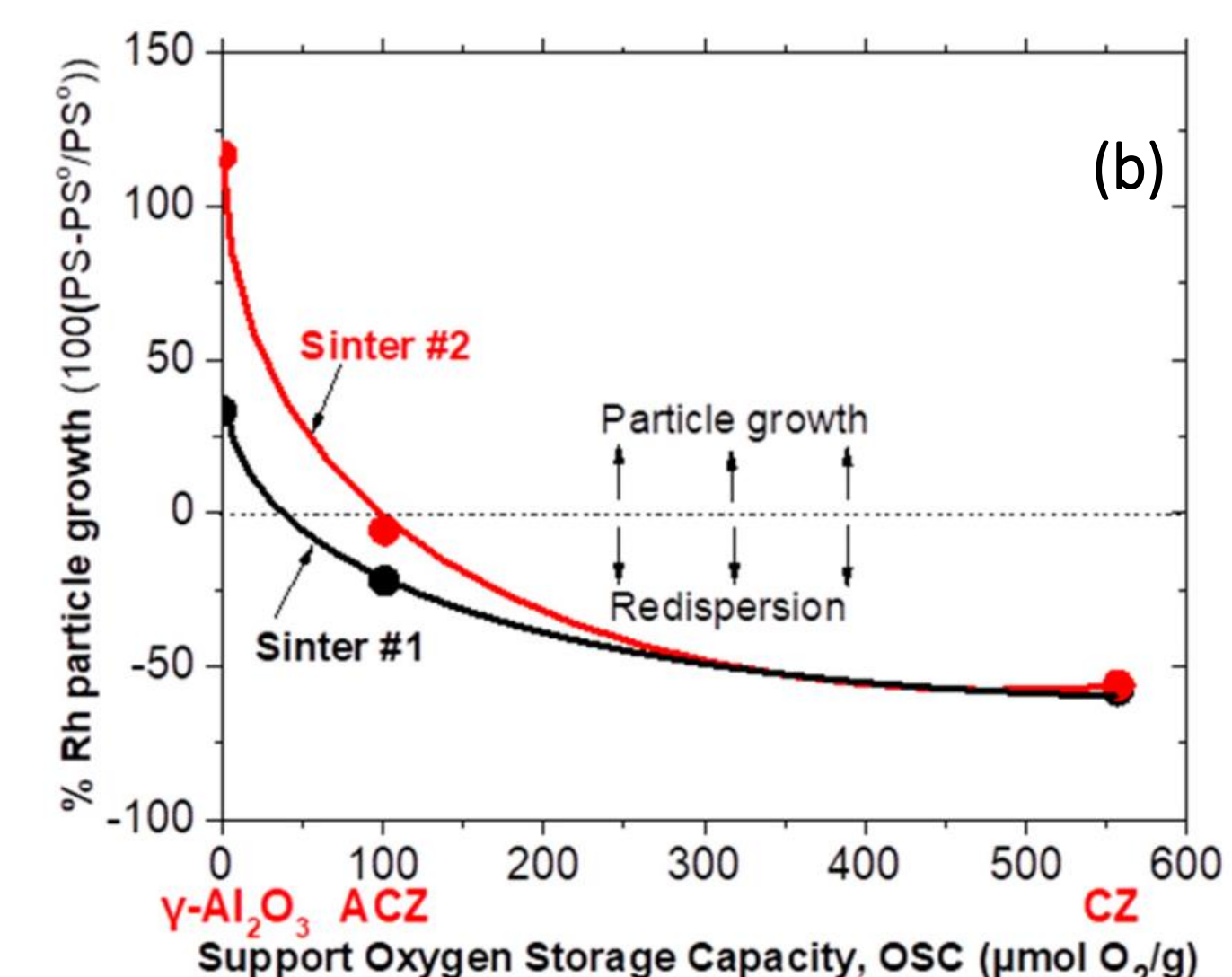
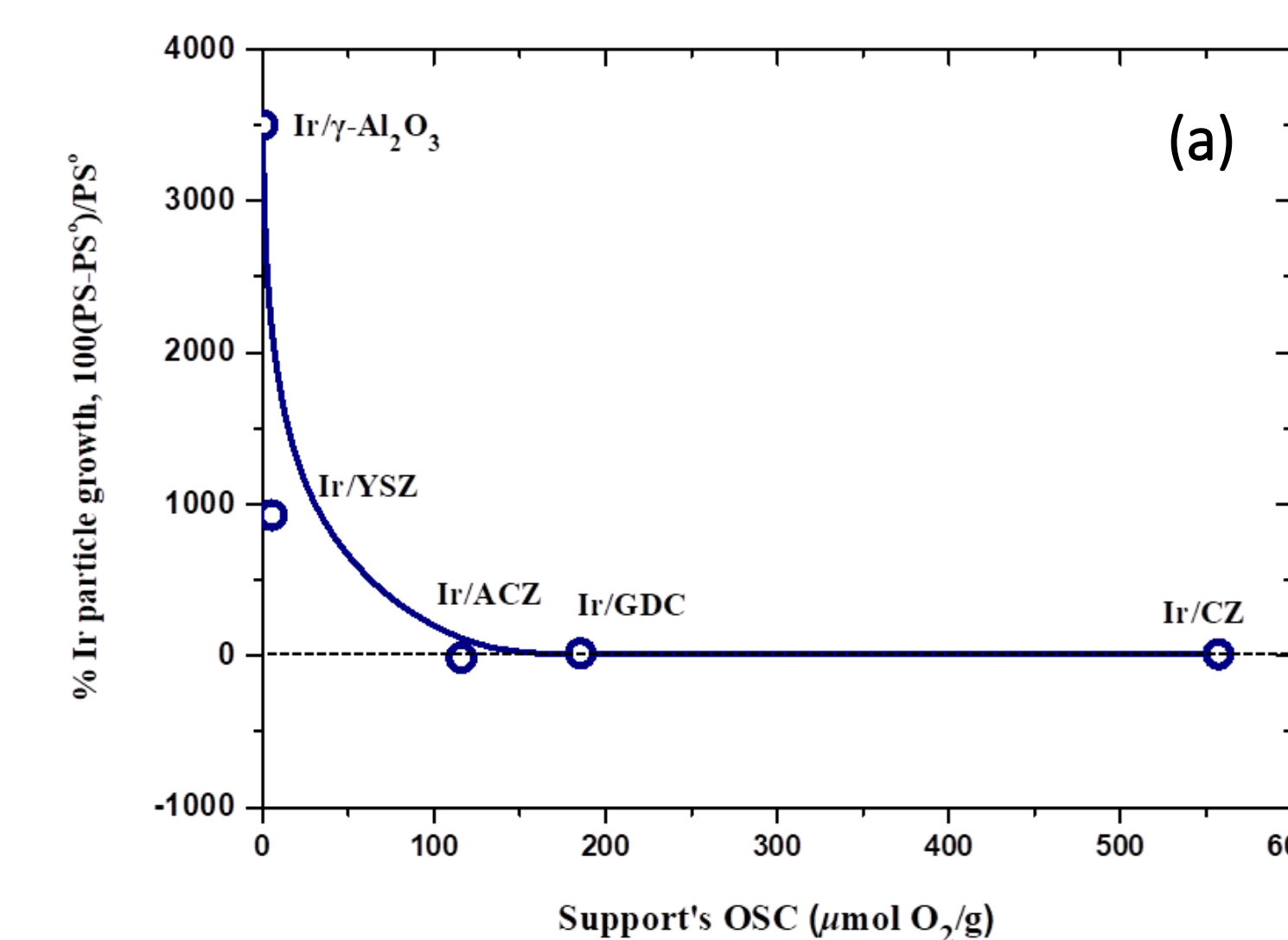


Fig. 5: Correlation of the sintering behavior (% particle growth) of supported Ir (a) and Rh (b) nanoparticles with the oxygen storage capacity (OSC) of the support [10,11]; positive "% particle growth" values indicate particles agglomeration, negative values indicate particles redispersion.

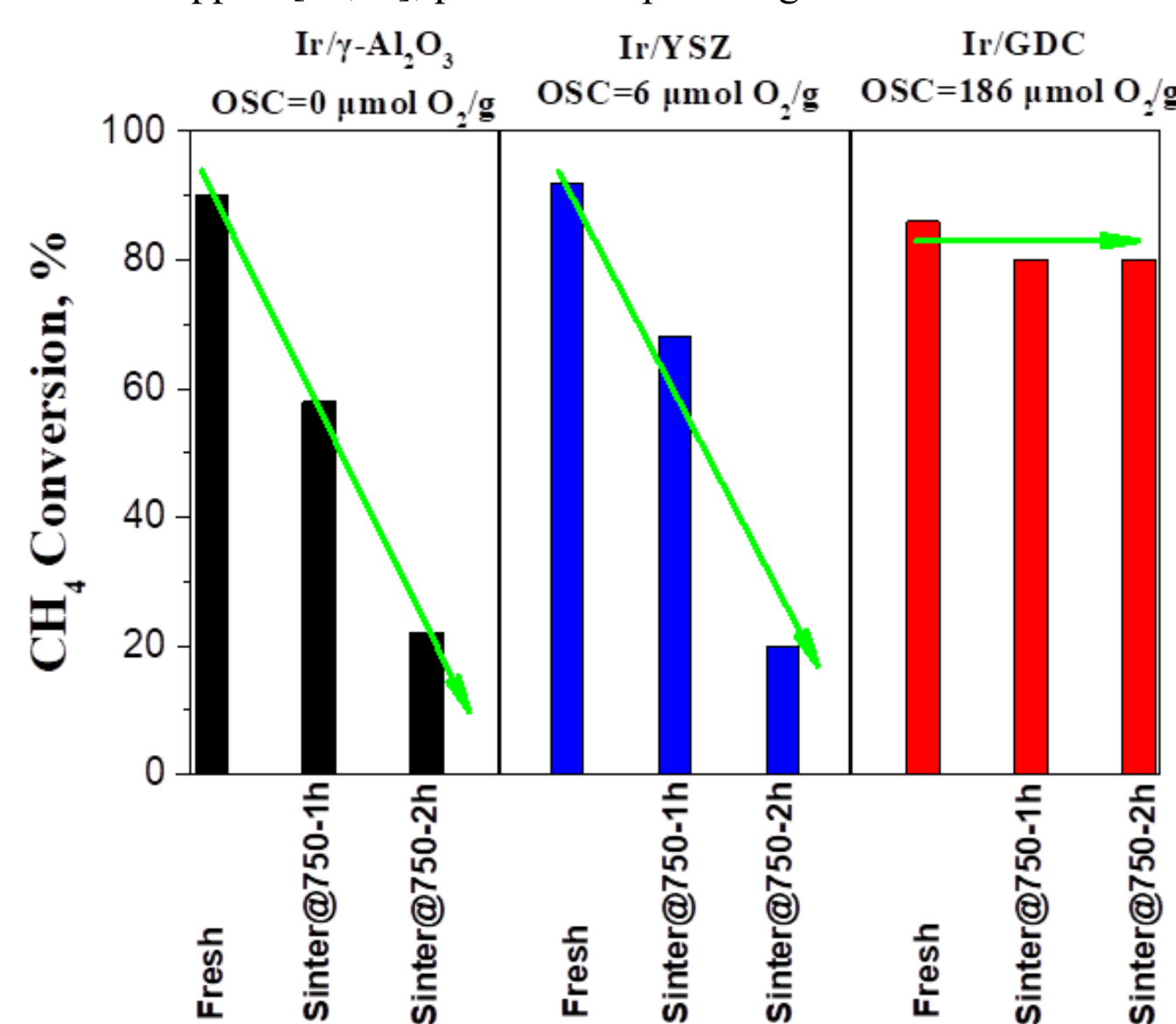


Fig. 6: CH_4 conversion efficiency of fresh and sintered Ir/ γ - Al_2O_3 , Ir/YSZ and Ir/GDC catalysts under DRM reaction at 750°C and $CH_4/CO_2=35.5\%/64.5\%$. Sinter@750-1h and Sinter@750-2h represent catalysts sintered in air flow at 750°C for 1 and 2 h [8].

4. Conclusions

- Supports with negligible OSC (e.g. γ - Al_2O_3 , YSZ) provided no or little resistance to sintering of catalyst nanoparticles dispersed on them
- In striking contrast, high resistance to sintering and even redispersion of catalyst nanoparticles resulted on supports characterized by moderate and high OSC values (e.g., ACZ, CZ and GDC).
- These findings provide a new methodology for sintering prevention or even in situ controlled redispersion of metal catalyst nanoparticles.
- A model has been developed convincingly explains the obtained experimental results.
- The new methodology of catalyst nanostructure stabilization and/or particle redispersion is of significant fundamental and practical importance for energy and environmental applications (e.g., Dry Reforming of methane reaction).

References

- Pliangos A, Yentekakis IV, Papadakis VG, Vayenas CG, Verykios XE. *Appl. Catal. B* 14 (1997) 161–173.
- Vayenas CG. *Catal. Lett.* 143 (2013) 1085–1097.
- Yentekakis IV, Vernoux P, Goula G, Caravaca A. *Catalysts* 9 (2019) 157.
- Vayenas CG, Bebelis S, Yentekakis IV, Lintz HG. *Catal. Today* 11 (1992) 303–442.
- Moulijn JA, van Diepen AE, Kapteijn F. *Appl. Catal. A* 212 (2001) 3–16.
- Argyle MD, Bartholomew CH. *Catalysts* 5 (2015) 145–269.
- Hansen TW, DeLaRiva AT, Challa SR, Datye AK. *Acc. Chem. Res.* 46 (2013) 1720–1730.
- Yentekakis IV, Goula G, Panagiotopoulou P, Katsoni A, Diamadopoulos E, Mantzavinos D, Delimitis A. *Top. Catal.* 58 (2015) 1228–1241.
- Yentekakis IV, Goula G, Panagiotopoulou P, Kampouri S, Taylor MJ, Kyriakou G, Lambert RM. *Appl. Catal. B: Environ.* 192 (2016) 357–364.
- Yentekakis IV, Goula G, Kampouri S, Betsi-Argyropoulou I, Panagiotopoulou P, Taylor MJ, Kyriakou G, Lambert RM. *Catal. Lett.* 148 (2018) 341–347.
- Goula G, Botzoulaki G, Osatiashtiani A, Parlett CMA, Kyriakou G, Lambert RM, Yentekakis IV. *Catalysts* 9 (2019) 541.
- Botzoulaki G, Goula G, Rontogianni A, Nikolaraki E, [...]. Yentekakis IV. *Catalysts* 10 (2020) 944.
- Nikolaraki E, Goula G, Panagiotopoulou P, Taylor MJ, Kousi K, Kyriakou G, Kondarides D, Lambert RM, Yentekakis IV. *Nanomaterials* 11 (2021) 2880.

Acknowledgements: This research has been co-financed by the European Union and Greek national funds through the Operational Program "Competitiveness, Entrepreneurship and Innovation", under the call "RESEARCH-CREATE-INNOVATE" (project code: T2EDK-00955).

